ORIGINAL PAPER

The energy threshold in dynamic probing

Sergio J. Ibanez[1] · Cesar Sagaseta[2] · Alfonso Fernandez del Rincon[3]

Abstract

In dynamic probing tests, penetration is closely related to the potential energy of the hammer (nominal energy). This energy stems from the mass and free fall of the hammer after being released from a certain height. Penetration depends on energy, although only on a portion of that nominal energy that is effectively transferred to the rods ($ENTHRU$) and, more precisely, the energy that reaches the cone ($ENTHRU_{cone}$). $ENTHRU$ can be measured by monitoring the upper part of the drive rods. To calculate $ENTHRU_{cone}$, $ENTHRU$ needs to be corrected in three ways. Firstly, the energy loss in the energy transmission through the rods has to be subtracted, as well as the energy loss due to the skin friction of the rods along the soil around them. It is also necessary to add the energy due to the rod weight penetrating the soil. The main hypothesis assumed and later experimentally proved in this paper is based on the fact that $ENTHRU_{cone}$ has to be greater than a certain value or minimum energy (energy threshold: T_h) in order to be able to cause penetration. After analyzing more than one hundred blows with different hammer mass and drop height, a small but consistent T_h and a linear relationship between energy and penetration beyond it were found. The energy that really produces penetration ($ENPEN$) will be $ENTHRU_{cone}$, minus T_h. This allows for improved energy corrections and correlations between results from various kinds of penetration tests.

Keywords Correlation · Penetration · Dynamic · Probing · Energy · Threshold

Introduction

Results from dynamic penetration tests are extensively used in geotechnical studies for calculating and designing purposes (Mishra and Robinson 2019). As there are many diverse types of dynamic penetration tests (Matsumoto et al. 2015), it is necessary to be able to correlate results among these various kinds of tests. The current formulas (Avanzi et al. 2013; Bergdahl 1979; Daniel et al. 2003; Hiley 1925) establish an inverse linear correlation between nominal energy and the number of blows (N). There is a market demand for improving these old, but widespread used correlations in order to make more accurate and efficient geotechnical designs. Current standards (ASTM 2016; ISO-AENOR-CEN 2005, 2011) also force geotechnical engineers to make energy corrections when using dynamic penetration test results. This article studies the penetration mechanism related to energy, proposing a new and improved way of correlating results among different kinds of dynamic penetration tests and a new equation for applying energy corrections to adjust blow counts to 60% energy efficiency.

Much effort has been made in the past (Abou-Matar and Goble 1997; Butler et al. 1998; Odebrecht et al. 2005; Sancio and Bray 2005; Schmertmann and Palacios 1979; Sy and Campanella 1991) to measure the parameters (force, acceleration, displacement and energy) involved in the Standard Penetration Tests (SPT), although studies on Dynamic Probing Tests (DP) have received less attention in specialized literature (Matsumoto et al. 2015; Michi et al. 2004; Žaržojus et al. 2013). The aim of the work presented in this paper is to reduce this gap, helping to understand the mechanism of the advance of continuous dynamic penetrometers. Some of the findings made for the SPT can be extended to DP; however, there are many substantial differences that require a specific study.

✉ Sergio J. Ibanez
  sibanez@ubu.es

1 Department of Architectonic Construction and Ground
   Engineering, Higher Polytechnic School, University
   of Burgos, Burgos, Spain

2 Department of Civil Engineering (ETS ICCP), University
   of Cantabria, Santander, Spain

3 Department of Structural and Mechanical Engineering,
   Faculty of Industrial and Telecommunication Engineering,
   University of Cantabria, Santander, Spain

Penetration is not only governed by soil characteristics, but also by the energy used by the penetration equipment. This penetration is not directly related to the whole potential energy of the hammer (nominal energy), but only to the portion of that energy that is effectively transferred to the rods (*ENTHRU*), as many authors state (Abou-Matar and Goble 1997; Butler et al. 1998; Daniel et al. 2003; Lee et al. 2014; Sancio and Bray 2005; Sy and Campanella 1991) and, more precisely, the energy that reaches the cone (*ENTHRU$_{cone}$*) (Anbazhagan et al. 2022; Lukiantchuki et al. 2017; Odebrecht et al. 2005; Schmertmann and Palacios 1979).

In practice, the interpretation of both SPT and DP tests is made by counting the number of normalized blows (N) needed for a given penetration length: 30 cm in SPT, 20 cm in DPSH-B, 10 cm in DPH, etc. (ISO-AENOR-CEN 2005, 2011). The nominal energy of each blow also varies across the different tests, albeit within a relatively narrow range. Typically, these values vary approximately between 300 and 500 J. If the DPM (medium dynamic probing) test is also considered, the range varies approximately between 150 and 500 J (ISO-AENOR-CEN 2005, 2011; Matsumoto et al. 2015).

As a first approximation, the comparison between the results using different penetrometers is based on a linear relation between the penetration per blow and the energy applied (Avanzi et al. 2013; Bergdahl 1979; Daniel et al. 2003). However, there are some non-linearities associated to energy losses at the hammer (Farrar 1998; Kovacs and Salomone 1982), the friction between the driving rods and the surrounding soil (Dahlberg and Bergdahl 1974), etc. Considerable advances (Dahlberg and Bergdahl 1974; Odebrecht et al. 2005; Schmertmann 2007) have been made to take them into account in a simple way while considering the nature of the phenomena involved.

However, there is a basic source of deviation (the existence of an energy threshold T_h) associated to the non-linearity of the stress–strain behavior of soils at small stresses. This is part of the assumption considered and further demonstrated throughout this research (Fig. 1). Nevertheless and in practice, a linear relation is assumed in a given soil between energy and penetration in the usual energy range for penetration tests (Avanzi et al. 2013; Bergdahl 1979; Daniel et al. 2003).

In this study, a conventional dynamic penetrometer has been instrumented by installing accelerometers and strain gauges at a point on the driving rods, which, after integration, allows the evolution of the applied energy during each blow of the hammer. The final permanent vertical tip displacement is measured by a caliper. The driving parameters (hammer weight and drop height) vary from blow to blow in order to get a full range of energies, with the tests performed on a site with uniform granular soil.

One of the results of the test campaign is that the relationship between useful energy and tip displacement
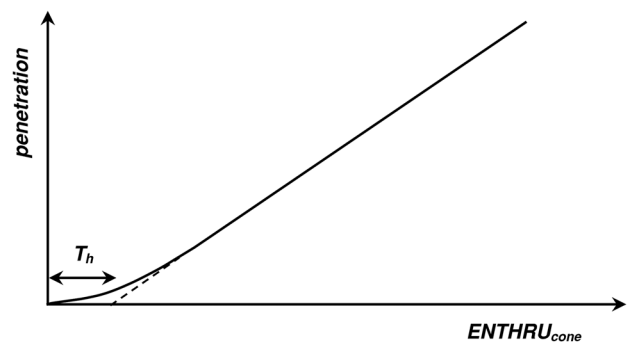

Fig. 1 Relationship between energy and penetration

(penetration) in each blow is approximately linear, but with an apparent energy threshold T_h below which no penetration occurs, as shown in Fig. 1.

The threshold T_h should be subtracted from the *ENTHRU$_{cone}$* to obtain the energy that really produces non-recoverable penetration (plastic displacement). This energy has to be used to correlate results among different dynamic penetration tests if a linear relationship between energy and penetration is assumed to be used, as it is in practice at present (Avanzi et al. 2013; Bergdahl 1979; Daniel et al. 2003). This T_h is not a real threshold, as the curve energy-penetration is not perfectly linear, especially for small energy values (Fig. 1); however, for the usual range of energies used in real penetrometers, the soil behaves as if such relationship was linear (see the dotted line in Fig. 1), but with an apparent energy threshold (T_h).

In summary, this paper sets out the development of a new adjusted method for correlating results from different kinds of dynamic penetrations tests, as well as offering a proposed new method for the energy correction requirement, taking into account the existence of the aforesaid T_h. A method for calculating this T_h is also proposed.

Energy efficiency

Many authors have been studying and measuring the energy balance when performing the SPT. The first studies covering this issue can be traced back to Palacios (1977) and Schmertmann and Palacios (1979), who measured energy transference by means of the use of strain gauges. Building on these first analysis, several authors followed this line of research during the next decades (Abou-Matar and Goble 1997; Butler et al. 1998; Farrar 1998; Lee et al. 2009; Odebrecht et al. 2005; Sancio and Bray 2005; Sy and Campanella 1991). During the last 10 years, it has still been a main theme in the field of in situ testing, with many other authors introducing very valuable observations (Anbazhagan et al. 2021, 2022; Lee et al. 2014, 2012; Look et al. 2015;

Lukiantchuki et al. 2017; Matsumoto et al. 2015). However, less attention has been paid to the analysis of the dynamic probing (DP) tests (Matsumoto et al. 2015; Michi 2004; Žaržojus et al. 2013). For this reason, the derivation of the dynamic equations for the cone penetrometers (DP) are made following the line of previous analyses for SPT.

Energy efficiency for SPT

Even though there are several studies regarding the measurement of energy in the SPT, this paper is consistent with one of the main recent investigations on this matter (Odebrecht et al. 2005). The methodology proposed by Odebrecht et al. (2005) has been used for several reasons, firstly, because this is one of the latest and most complete pieces of research on energy measurement in penetration testing. In the authors' opinion, this approach is the most appropriate to apply to this research, since it considers the real energy that reaches the bottom part of the rod assembly, i.e., the cone ($E_{sampler}$), unlike other methods of operation that consider only the energy transmitted to the upper part of the rods (close to the anvil). Thus, by using this methodology, it has been possible to include the additional potential energy due to the mass of the rods and the hammer during penetration displacement, with every energy loss considered during transmission of the energy through the rods.

Housel (1965) was the first to use the term *ENTHRU*, that is, the energy transmitted to the rod stem. *ENTHRU* has been measured by means of integrating signals from some accelerometers and strain gauges located below the anvil, as is usual in such tests.

Some authors (Daniel et al. 2003) have used this *ENTHRU* in order to correlate results from different types of tests.

Odebrecht et al. (2005) found that *ENTHRU* could be expressed through this equation:

$$ENTHRU = \eta_1 \cdot m_h \cdot g \cdot (h + p) \tag{1}$$

where η_1 is the hammer efficiency factor, m_h represents the hammer mass, g is the gravity acceleration, h is the height of fall (free fall of the hammer after being released), and p is the permanent penetration per blow.

After analyzing the data from the tests using Schedule 80 rods, pursuant to the Brazilian Standard (NBR-ABNT 2001), the value of η_1 yields 0.765.

Odebrecht et al. (2005) also inferred the value of the computed sampler energy ($E_{sampler}$), the value of the actual energy that reaches the sampler.

$$E_{sampler} = \eta_3 \cdot \left[\eta_1 \cdot m_h \cdot g \cdot (h + p) + \eta_2 \cdot m_r \cdot g \cdot p \right] \tag{2}$$

where η_3 represents the energy efficiency factor, η_2 is the rod efficiency factor, and m_r is the rod mass.

The adjusted experimental data and the proposed values for the efficiency factors were:

$$\eta_3 = 1 - 0.0042 \cdot l \tag{3}$$

where l is the rod length (m).

The value of η_2 equals 1.

Differences between SPT and DP tests

Both kinds of tests are quite similar although there are some differences that will have to yield to different approaches to the measurement of the energy.

Firstly, the DP tests are performed continuously along the depth, whereas in the case of SPT, the tests are conducted only at certain points inside a borehole that is perforated using different methods (Fig. 2). As this research is fully devoted to Dynamic Probe (DP) testing, the base scenario for this investigation will be the second configuration shown in Fig. 2.

SPT tests are carried out with a sampler of a smaller diameter than the borehole casing, driven into the soil, allowing a disturbed sample to be taken. The bottom of the borehole, inside and around the sampler, is a free boundary. On the contrary, in the DP tests, the hole is created by the cone itself, with no horizontal free boundary at the bottom. On the other hand, there is no casing, meaning that the vertical walls can deform and exert a certain radial pressure and hence friction on the rods.

Materials and methods

Due to the differences between SPT and DP tests, a new method for calculating energy efficiency in DP tests shall be proposed. It is important to highlight that there are many studies that calculate energy efficiency in SPT tests; however, there are very few studies on energy efficiency in DP tests.

Such energy efficiency has to be used to correlate results among different DP tests. For this purpose, it is good practice to use the real energy that produces penetration. An improvement will be proposed in the use of such correlations, considering that an energy threshold (T_h) may exist which has to be exceeded to produce penetration.

This is the key factor of the present paper and the existence of this T_h will be demonstrated throughout this research.

Measuring lateral friction

The drive rods and the cone will be driven vertically in order to avoid lateral friction. This is of particular relevance in dense

Fig. 2 Geometrical differences between SPT and DP
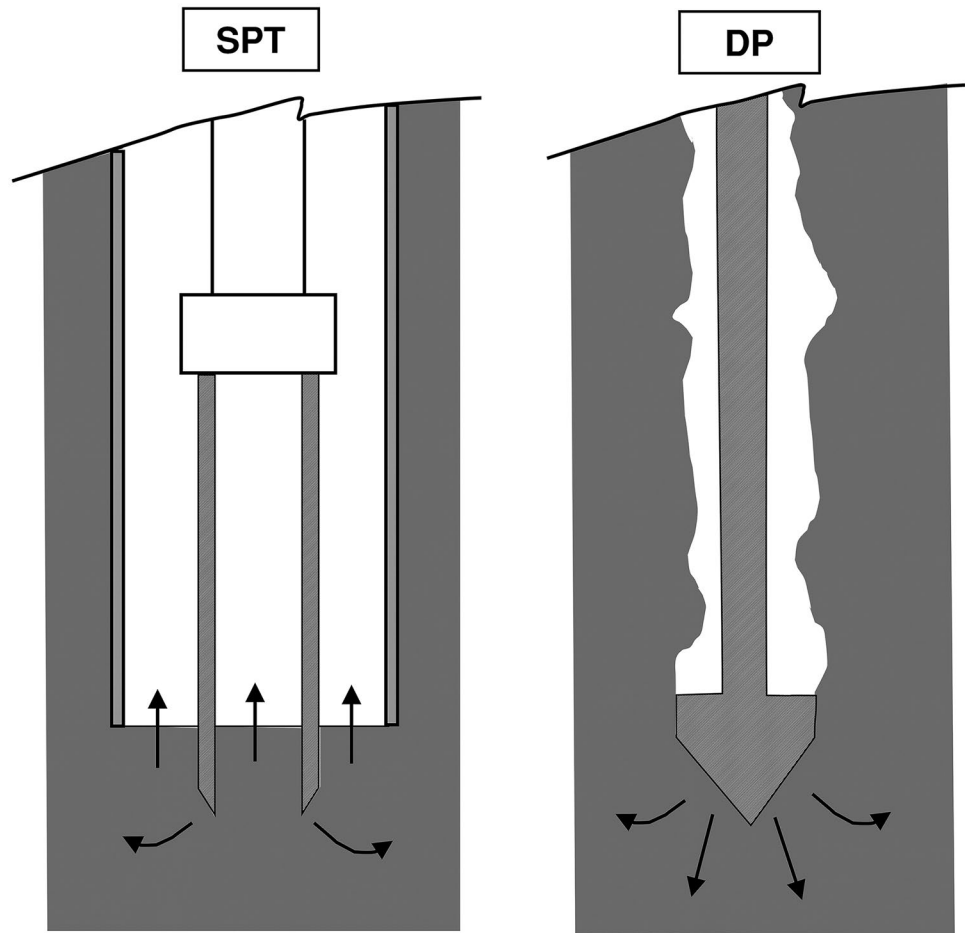
sands and cohesive soils at depth (Cearns and McKenzie 1988).

Rods are rotated 1.5 turns or until maximum torque is reached at least at every 1-m penetration. The aim of this rotation is to tighten the rod connections and to reduce skin friction.

Every dynamic probing equipment has its torque measuring system which usually involves a torque wrench or similar device. Rods are rotated by means of this device, meaning that the value of the maximum torque is obtained at the same time.

The frictional force F_f, necessary to rotate the drive rods, is calculated through the skin resistance and the lateral area of the drive rods.

$$F_f = \tau \cdot 2 \cdot \pi \cdot r \cdot l \qquad (4)$$

where τ represents skin friction resistance, r is the rod radius, and l is the rod length.

The maximum torque necessary to rotate the drive rods will be the frictional force multiplied by the rod radius.

$$T = F_f \cdot r = \tau \cdot 2 \cdot \pi \cdot r^2 \cdot l \qquad (5)$$

where T is the maximum torque.

The value of the skin friction is thus calculated by Eq. (6) below:

$$\tau = \frac{T}{2 \cdot \pi \cdot r^2 \cdot l} \qquad (6)$$

The energy used to overcome the friction between the drive rods and the soil around them during penetration (frictional energy E_f) can be calculated by means of Eq. (7):

$$E_f = F_f \cdot p \qquad (7)$$

Substituting the value of F_f from Eq. (4) in Eq. (7):

$$E_f = \tau \cdot 2 \cdot \pi \cdot r \cdot l \cdot p \qquad (8)$$

In addition, by using the value of the skin friction from Eq. (6), we get the final Eq. (9):

$$E_f = \frac{T \cdot p}{r} \qquad (9)$$

This Eq. (9) was obtained by Dahlberg and Bergdahl (1974).

The aforementioned equation only works when assuming that quasi-static skin friction during rotation of the drive rods is the same as the dynamic skin friction during penetration.

Due to this difference between skin friction in static and dynamic processes, Bergdahl (1979) calculated the part of the total number of blows in a penetration test that was "used" to overcome that lateral friction (Nixon 1988; Scarff 1988). Bergdahl (1979) then measured the energy due to lateral friction and found that it was the same energy shown in Eq. (9), but with an empirical correction factor of 3.4. This means that dynamic lateral friction resistance in a vertical direction during driving is much greater than semi-static resistance in a horizontal direction during the turning of the rods. When calculating that factor, Bergdahl (1979) was assuming 100% energy efficiency, meaning that in this research it will be necessary to multiply that energy by the energy efficiency factor (η).

We can thus consider the next equation to arrive at that frictional energy:

$$E_f = \frac{T \cdot p}{r} \cdot 3.4 \cdot \eta \tag{10}$$

where η represents the energy efficiency factor.

This efficiency means the percentage out of the nominal energy that reaches down to the cone.

Nominal energy is defined as the hammer weight multiplied by the height of fall.

$$E_f = \frac{T \cdot p}{r} \cdot 3.4 \cdot \frac{E_{sampler}}{m_h \cdot g \cdot h} \tag{11}$$

$ENTHRU_{cone}$ in DP tests

In the rest of this paper, $ENTHRU_{cone}$ is defined as the real amount of energy that effectively reaches the cone in DP tests (Ibanez et al. 2012). It is the equivalent to what Odebrecht et al. (2005) called $E_{sampler}$ in a SPT test.

By using the $E_{sampler}$ in a SPT (Eq. (2)) as part of the new $ENTHRU_{cone}$, it is necessary to subtract that part of the $ENTHRU$ that is used to overcome that skin friction (E_f) from $E_{sampler}$ (Matsumoto et al. 2015). Equation (12) is thus obtained:

$$ENTHRU_{cone} = \eta_3 \cdot \left[\eta_1 \cdot m_h \cdot g \cdot (h+p) + \eta_2 \cdot m_r \cdot g \cdot p \right] - E_f \tag{12}$$

By substituting the value of E_f (Eq. (11)) in Eq. (12), and knowing that η_2 equals 1:

$$ENTHRU_{cone} = \eta_3 \cdot \left[\eta_1 \cdot m_h \cdot g \cdot (h+p) + m_r \cdot g \cdot p \right] \cdot \left(1 - \frac{T \cdot p \cdot 3.4}{r \cdot m_h \cdot g \cdot h} \right) \tag{13}$$

The value of m_r is the mass of the rods, although it would be better to also include the anvil mass. Odebrecht et al. (2005) took into consideration the additional potential energy delivered to the cone due to the weight resting on the sampler (cone for DP tests) along the penetration p. In DP testing, not only the mass of the rods and the mass of the hammer acts on the cone, but also the anvil rests on the cone, meaning that the anvil mass has to be included. In this regard, if there were any mass additional to the hammer mass, rod mass, or anvil mass that was resting on the cone during penetration, this should be also included in the anvil mass. Equation (13) can thus be rewritten:

$$ENTHRU_{cone} = \eta_3 \cdot \left[\eta_4 \cdot m_h \cdot g \cdot (h+p) + m_a \cdot g \cdot p + m_r \cdot g \cdot p \right] \cdot \left(1 - \frac{T \cdot p \cdot 3.4}{r \cdot m_h \cdot g \cdot h} \right) \tag{14}$$

where m_a is the mass of the anvil where the hammer strikes when falling and η_4 represents the energy efficiency factor.

This different way of measuring $ENTHRU$ makes η_1 different to η_4, as Odebrecht et al. (2005) calculated η_1 by means of the $ENTHRU$, disregarding the value of m_a. Therefore, in dynamic probing (DP tests), we cannot assume the value of η_4 as 0.765 as Odebrecht et al. (2005) stated.

In compliance with ISO-AENOR-CEN (2005, 2011), as can be seen in Fig. 3, $ENTHRU$ (Eq. (15)) is measured just below the anvil but at a distance a little greater than 10 times the rod diameter below the point of hammer impact:

$$ENTHRU = \eta_4 \cdot m_h \cdot g \cdot (h+p) + m_a \cdot g \cdot p \tag{15}$$

Schmertmann and Palacios (1979) found that the hammer remains in contact with the rods for only about 25% of the penetration (Schmertmann 2007). Equation (15) does not include this correction. This is not a real problem in this research, as $ENTHRU$ will actually be measured through monitoring.

Equation (14) can be rewritten as:

$$ENTHRU_{cone} = \eta_3 \cdot \left(ENTHRU + m_r \cdot g \cdot p \right) \cdot \left(1 - \frac{T \cdot p \cdot 3.4}{r \cdot m_h \cdot g \cdot h} \right) \tag{16}$$
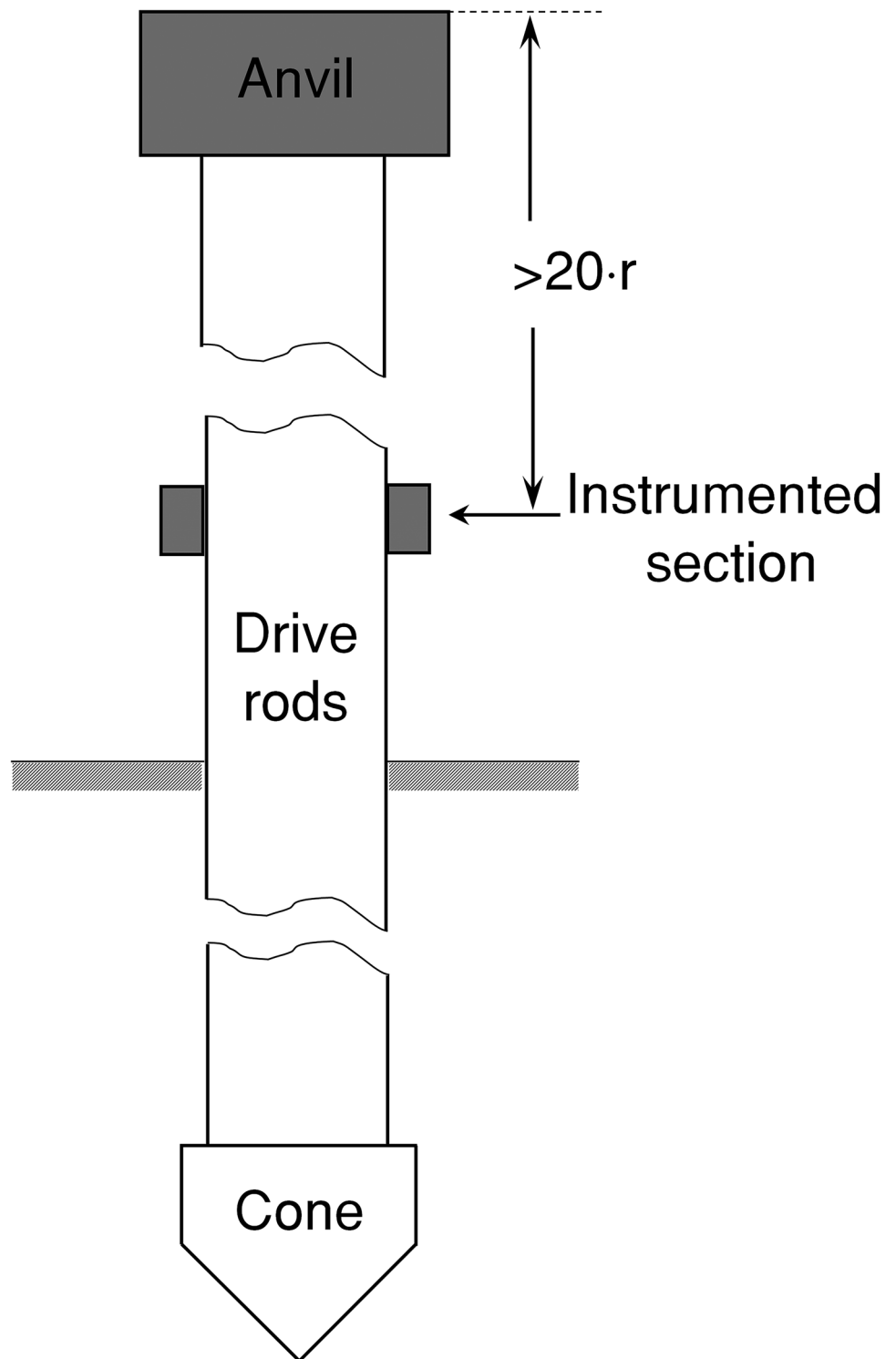
The value of η_3 obtained from Eq. (3) will be changed. It would be better if this factor were expressed in non-dimensional form.

If the last part of this factor is multiplied and divided by the rod radius:

$$\eta_3 = 1 - 0.0042 \cdot l \cdot \frac{r}{r} \tag{17}$$

The rods used by Odebrecht et al. (2005) had the normal radius for SPT (1.14×10^{-2} m).

Fig. 3 Instrumented rod (ISO-AENOR-CEN 2005, 2011)

$$\eta_3 = 1 - 0.0042 \cdot l \cdot \frac{1.14 \cdot 10^{-2}}{r} = 1 - 4.8 \cdot 10^{-5} \cdot \frac{l}{r} \quad (18)$$

This way of computing η_3 is such that it has been assumed that the greater radius of rod, the greater the stiffness of the rod stem, resulting in greater energy efficiency. This research has also been performed by using values taken directly from Eq. (3), with fairly comparable results and conclusions that are identical to this research thus obtained. Hence, it is preferable to use this factor, as shown in Eq. (18).

$ENTHRU_{cone}$ is therefore finally obtained as:

$$ENTHRU_{cone} = \left(1 - 4.8 \cdot 10^{-5} \cdot \frac{l}{r}\right) \cdot \left(ENTHRU + m_r \cdot g \cdot p\right)$$
$$\cdot \left(1 - \frac{T \cdot p \cdot 3.4}{r \cdot m_h \cdot g \cdot h}\right) \tag{19}$$

Energy threshold

The current formulas (see Eq. (20)) used to correlate results among the different dynamic penetration tests establish an inverse linear correlation between nominal energy and the number of blows (N). This equation has been proposed in the ESOPT Symposium in 1974 (originating from the Dutch Formula (Bergdahl 1979) and Hiley's Formula (Hiley 1925)) and is currently used in geotechnical engineering (Avanzi et al. 2013). This means that it may be possible to compensate a very little amount of energy in each blow by means of a large number of blows in order to achieve the same penetration. However, it is obvious that by using an extremely small amount of energy per blow, it is not possible to cause any penetration at all.

$$N_1 = N_2 \cdot \frac{m_2 \cdot g \cdot h_2 \cdot A_1 \cdot e_1}{m_1 \cdot g \cdot h_1 \cdot A_2 \cdot e_2} \tag{20}$$

where A is the cross-sectional area of the cone and e is the total penetration during the test. This Eq. (20) relates results from two different DP tests: 1 and 2 (used as subscripts).

If possible, this Eq. (20) should be better used in terms of $ENTHRU$, instead of by using nominal energies (Daniel et al. 2003).

Some studies (Daniel et al. 2005; Danziger et al. 2006) argue that some secondary impact may still be able to contribute to cone penetration, while others saw different results from their research with no further penetration due to secondary impacts (Schmertmann and Palacios 1979). In fact, a number of more recent studies (Lee et al. 2014, 2009) have concluded that some secondary impact and subsequent events, such as low energy impacts, do not produce further penetration.

It is assumed that it is necessary to exceed a certain level of energy to produce penetration (Ibanez 2009), referred to as the "energy threshold" (T_h). This idea was originally conceived by Sanchez-Alciturri, J.M. during his mentoring for a doctorate (Ibanez 2009). Similar results, in terms of force (Soriano 1994), establish that a force (of the compression wave) greater than a certain value (half the dynamic resistance of a soil) to really cause penetration is required.

The Hiley formula (Hiley 1925) for pile capacity also states that there is a resistance to penetration called the ultimate driving resistance of the soil (R_u).

Thus, a new term is defined: $ENPEN$, which is the ENergy that actually produces non-recoverable PENetration into the soil:

$$ENPEN = ENTHRU_{cone} - T_h \tag{21}$$

If a single penetration test is performed and all the recorded blows are compared with each other, penetration p in terms of depth (p/C_N) has to be corrected. In other words, the penetration calculated in this way is the penetration obtained if all the blows had been performed at the same depth (at which the effective vertical stress approximately equals 100 kPa). The overburden correction factor (C_N) used was proposed by Liao and Whitman (1986). We shall therefore use this corrected penetration ($p*$):

$$p* = \frac{p}{C_N} \tag{22}$$

If T_h existed and there were a linear relationship between $ENTHRU_{cone}$ and corrected penetration ($p*$) beyond that T_h (conclusion that can be directly derived from Eq. (20)), it would be easy to calculate this T_h. If a large amount of data from blows in the same homogeneous soil is plotted in terms of $ENTHRU_{cone}$ vs. $p*$, T_h would be the x-intercept (see Fig. 1). In other words, T_h would be the energy that, if it is not surpassed, will mean there is no penetration at all.

In fact, this is just further evidence of the widely accepted non-linearity of soil behavior for very small strains. As will be shown later, behavior in the range of usually applied energies is roughly linear, with this non-linearity only appearing for extremely low values of $ENTHRU$.

In the same way as the energy efficiency in dynamic penetration tests depends on the stiffness of the soil, as has been demonstrated in the latest research (Look et al. 2015; Matsumoto et al. 2015; Žaržojus et al. 2013), this T_h would also be related to this stiffness.

Physical analysis of the energy threshold

At every blow, there is a force (F) that acts on the cone against the soil below. This F produces a penetration, or displacement of the cone (s), which consists of an elastic displacement and a plastic displacement. This latter displacement is the vertical displacement measured by a caliper (p). The elastic displacement just before failure shall be called s_0. Figure 4 shows the behavior of a perfectly plastic model (Briaud 2013).

$ENTHRU_{cone}$ will be the work exerted by this force during driving:

$$ENTHRU_{cone} = \int F \cdot ds \tag{23}$$

Considering the elastic behavior of the soil, and its stiffness (k):

$$F = k \cdot s \qquad (24)$$

If $F < R_u$:

$$ENTHRU_{cone} = \int k \cdot s \cdot ds = \frac{1}{2} \cdot k \cdot s^2 = \frac{1}{2} \cdot \frac{F^2}{k} \qquad (25)$$

However, if $F = R_u$, then there is a plastic displacement (p):

$$ENTHRU_{cone} = \frac{1}{2} \cdot \frac{R_u^2}{k} + R_u \cdot p \qquad (26)$$

The meaning of Eq. (26) is such that there is an energy threshold (T_h), the value of which is:

$$T_h = \frac{1}{2} \cdot \frac{R_u^2}{k} \qquad (27)$$

When the T_h is reached, $ENTHRU_{cone}$ increases linearly with a slope R_u. As we are going to use p^* instead of p, the slope will be $R_u \cdot C_N$, as shown in Eq. (22). As the result of this physical analysis, the $ENTHRU_{cone}$-p^* relationship is depicted in Fig. 5. In this case, the slope is the reciprocal of $R_u \cdot C_N$. C_N is going to be calculated as the medium value at the considered depth under study.

Field testing

All the foregoing considerations show the need to validate those hypotheses by means of a broad field testing with real energy measurements.
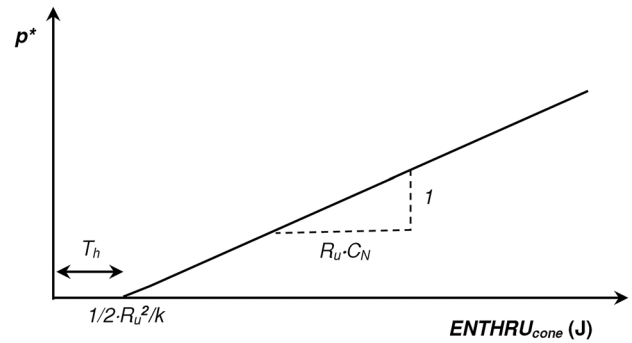

Fig. 5 $ENTHRU_{cone}$-p^* relationship

More than one hundred blows were given using an instrumented rod in order to calculate the value of T_h, according to Eq. (21) (the x-intercept in the graph $ENTHRU_{cone}$ vs. p^*, as can be seen in Figs. 1 and 5).

For each blow, the energy ($ENTHRU$), the depth, and the real penetration were measured. $ENTHRU_{cone}$ was calculated by means of Eq. (19).

Field site

The field work was conducted at Arija, in the north of the province of Burgos, Spain. Figure 6 shows the location of this site and a detailed orthophoto.

The geotechnical profile at the site includes a 40-m-thick sedimentary layer of Holocene deposits, containing rock fragments, siliceous minerals with a sizeable quantity of feldspars, micas, some heavy minerals, iron oxides, and carbonates. The bedrock is formed by sandstone and siltstone clay from the Cretaceous period.
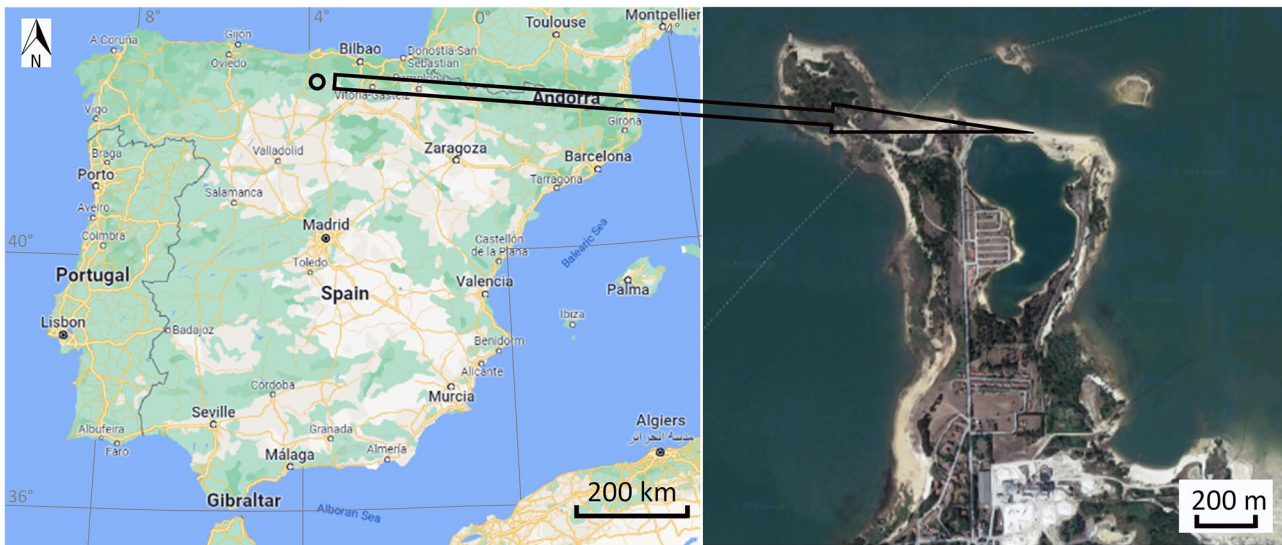
Fig. 4 Force vs. Displacement
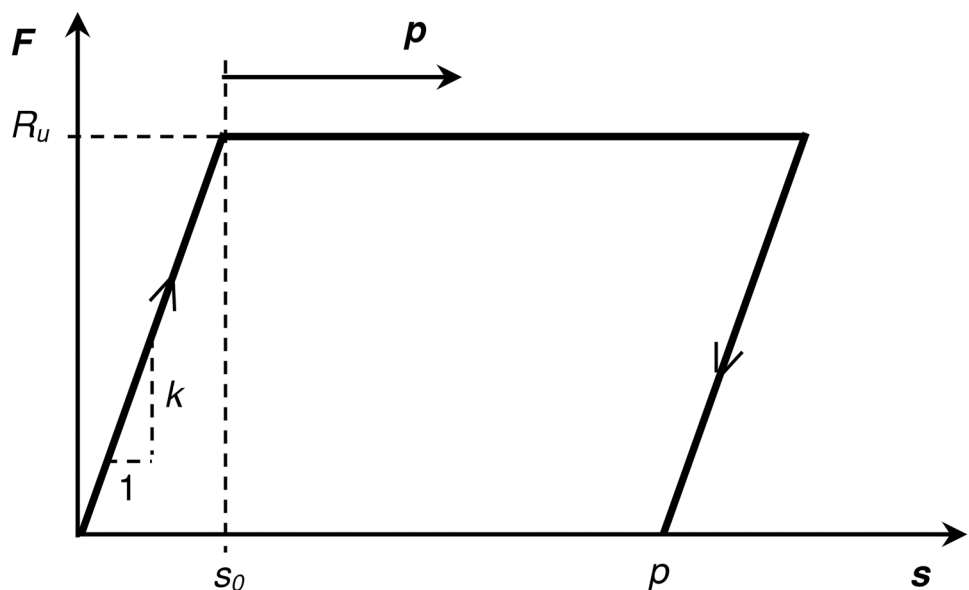
Fig. 6 Location and orthophoto (latitude and longitude: 43.00328, −3.94099) (mapping from Google Maps)

The upper 6.5 m of soil is a uniform clean silica sand (classified as SP, USCS), with a particle size distribution curve as shown in Fig. 7 and a bulk unit weight of 19.8 kN/m³. Below this level, the clay content increases.

These sands are of a great economical interest and they are dragged out from the river for construction and industrial purposes.

The soil surface was relatively horizontal and it was easy to access with all the equipment (a penetrometer on wheels and vehicle).
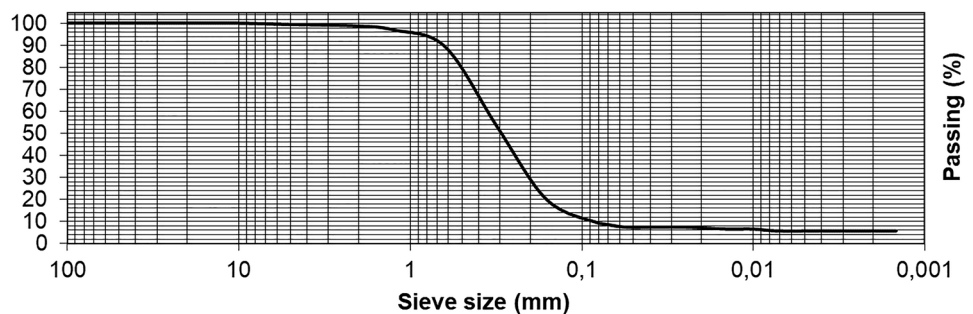
Geotechnical survey

The blows, the results of which will be used in this research, were performed at the location P in Fig. 8, with a geotechnical survey designed to geotechnically characterize the site. A series of geotechnical in situ and laboratory tests were performed around P.

Around P, three penetration tests (DPSH-B) were also performed, forming an equilateral triangle whose sides are 3 m long (as can be seen in Fig. 8). The results of these DPSH-B tests (N_{DPSH-B}) can be also seen in Fig. 13.

Electrical resistivity tests were also performed because, in the authors' opinion, it is important to get more information regarding the stratigraphic profile of the site (it was especially important to know where the clean and clayey sands were located). This research was originally designed to perform tests at different depths, meaning that it was considered indispensable to get more information on the layer profile to better choose at what depth the DP tests were going to be carried out. By means of these electrical profiles, it was decided to perform one of the sets of tests at a depth of below 6.5 m, where the clayey sands were located. Finally, in combination with the results from DPSH tests, it was decided to conduct one of the sets of tests at a depth of between 6.7 and 7.0 m, as will be explained later.

As a two-dimensional soil profile was required, the ERT (electrical resistivity tomography) method was chosen. An electrical resistivity test was therefore conducted passing through P, using a Schlumberger-Wenner configuration. The geometry of the electrodes defines the array, of which there are several kinds, with the most common being the dipole–dipole and Schlumberger-Wenner configurations. For the expected soil profile (approximately horizontal layers),
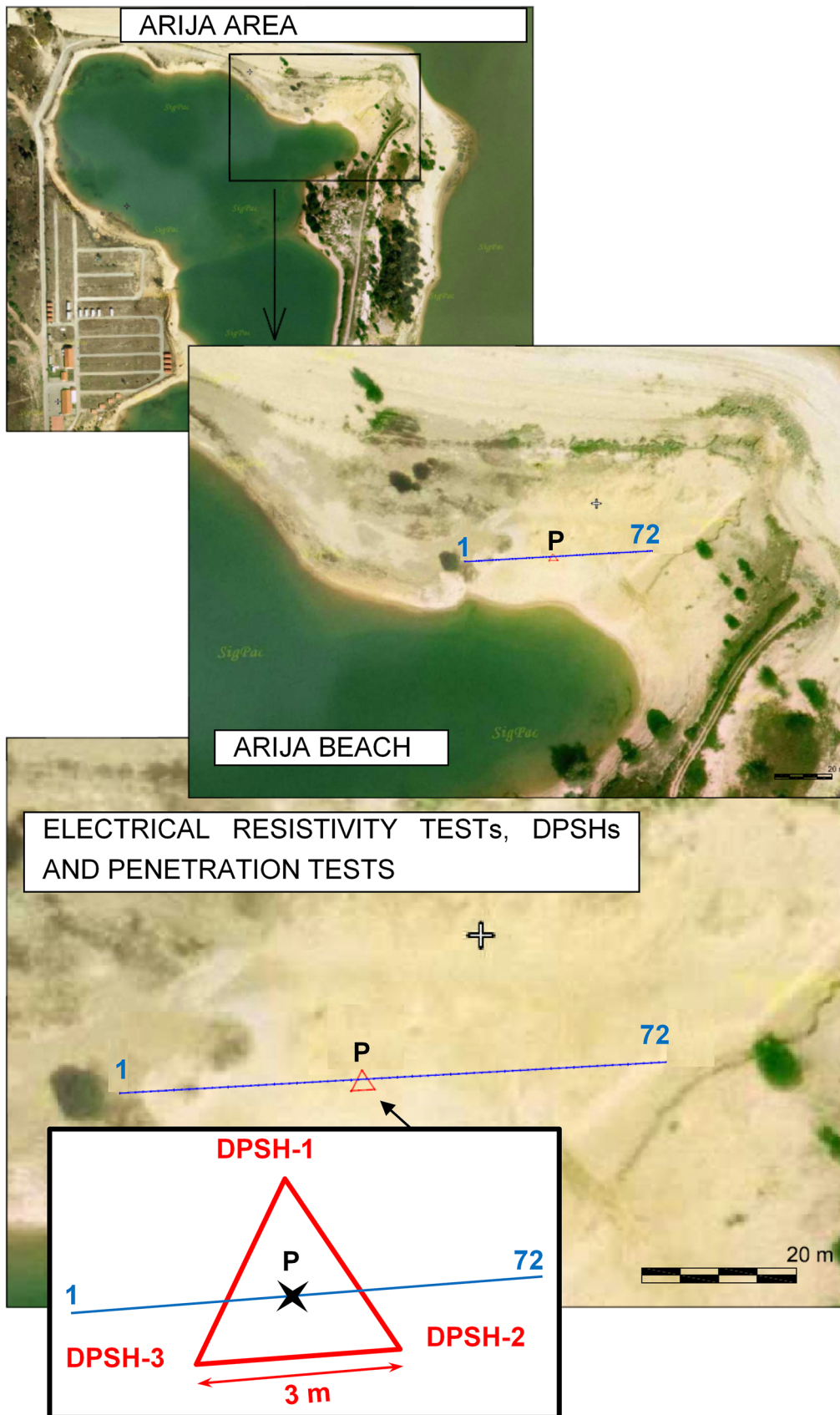
Fig. 7 Grain size distribution curve

Fig. 8 Geotechnical survey (Aerial photos from SIGPAC, Fondo Español de Garantía Agraria O.A.–FEGA)

the Schlumberger-Wenner array is the one which offers the best results (Pazdirek and Blaha 1996).

The electrical resistivity survey was undertaken using a SYSCAL R1 PLUS Switch72 device, property of the University of Burgos. The electrical tests were designed with the processing software ELECTRE (a total of 1,313 electrical measurements were conducted along the cross section). After rejecting invalid quadripole data, the apparent electrical resistivity cross section was plotted using PROSYS II processing software. RES2DINV interpretation software was used for inversion of the 2D ERT data for calculating real electrical resistivity cross sections (Fig. 9).

As a high density of data was preferred to going very deep, electrode spacing used was small (1 m) (Fig. 9 Profile a). The test was repeated at the central part, closer to P, but with a smaller electrode spacing (0.5 m) (Fig. 9 Profile b) to get even a higher resolution near P.

The results from the electrical resistivity tests are shown in Fig. 9. The geological interpretation is such that the shallower part of the soil consists of a layer of clean sands. Below a depth of approximately 5.5–6.5 m, the electrical resistivity of the sands becomes smaller. It is interpreted as the sand increases its clay content.

By trying to better characterize these shallower clean sands, two direct shear tests were also performed, with the sand compacted to the real in situ unit weight. The values of the critical and peak shear strength are shown in Fig. 10. The failure envelope for either critical ($\phi = 29°$) and peak ($\phi = 35°$) values is also depicted.

Direct shear tests were carried out on these dilatant sands until the ultimate condition was reached at large strains. After the peak, deformations occurred, with a quite appreciable softening. When there was not any further change of volume, the specimen reached the critical condition. These values of shear stresses at large deformations are the critical values, which define the critical state line (Lancellota 1995).

The depth of the ground water level varied from 0.4 to 0.9 m during the period of the field campaign.

Dynamic penetration apparatus and adjustments

The field campaign was carried out using DPSH-B equipment (a Sunda Menhir 100 kN-DPSH penetrometer), with a standard r value (1.14 cm). The cross-sectional area of the cone (A) was 20.03 cm^2.

This wheeled DP apparatus has to be transported by vehicle. In this case, an off-road vehicle was used (Fig. 11).

The Sunda penetrometer is prepared to be used for DPSH-B and DPSH-A (in such a case, just by taking down the hammer height magnetic controlling sensor a total of 25 cm). DPM tests can also be undertaken. In this case, not only the sensor has to be taken down 25 cm, but the hammer has to be replaced by a 50-kg hammer (also provided with the original penetrometer).

Pursuant to ISO-AENOR-CEN (2005, 2011), the instrumented section was located at a distance of 32.6 m from the top of the anvil (greater than ten times the diameter of the bars). A schematic figure of penetrometer can be seen in Fig. 11.

The aim of this research is to perform different DP tests and plot their results in figures such as Figs. 1 and 5 in order to find out if T_h really exists or not. There is therefore

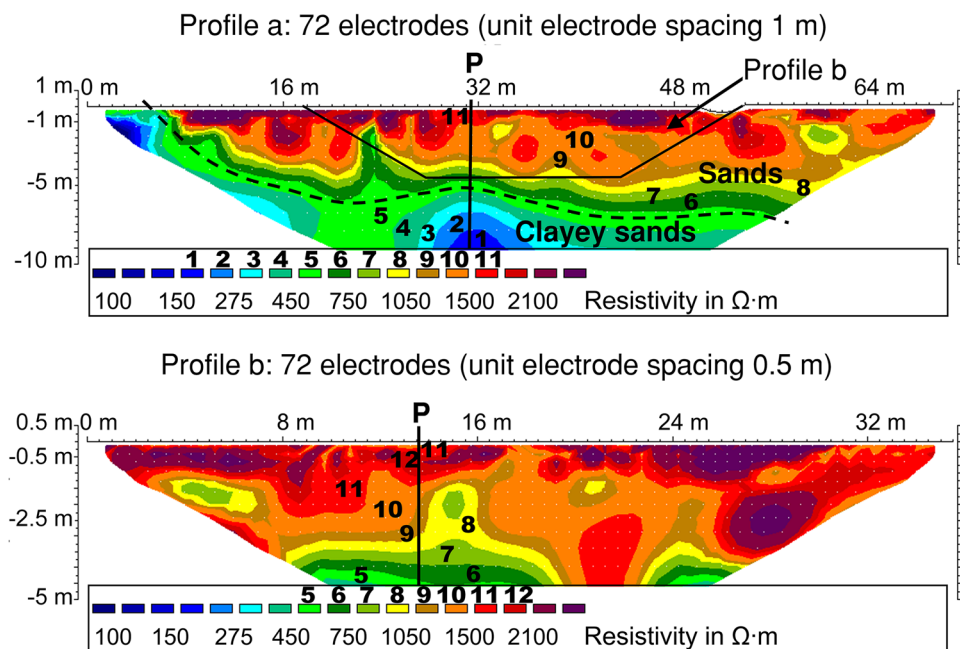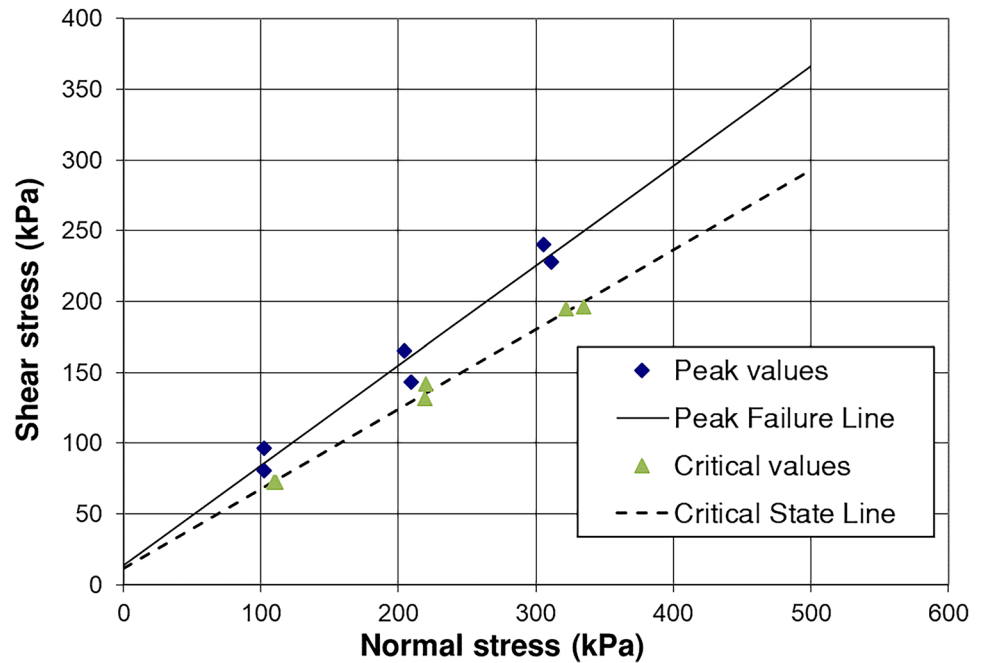**Fig. 9** Electrical resistivity tests

Fig. 10 Direct shear tests

a need to perform tests in which different $ENTHRU_{cone}$ are obtained. Due to the latter, the penetrometer was adapted for being able to perform tests in which the nominal energies could be easily changed.

Nominal energies can be transformed either by changing the height of fall or the mass of the hammer.

In such a way, the dynamic penetrometer was first modified in order to be able to change the height of fall. This was fairly easy, as it just consisted of changing the location of a magnetic sensor, by drilling the support bar where the sensor is attached (see Fig. 12). In this manner, the height of fall of the hammer could be chosen from 40 to 75 cm (every 5 cm).

The original hammer was then replaced by another smaller hammer and a series of additional steel plates that could be bolted to the hammer or not, as can be seen in Fig. 12. This new hammer and steel plates should fulfill some geometrical requirements of the penetrometer architecture.

By combining and assembling different number of these steel plates, we found hammer mass ranging from approximately 40 to 70 kg. It is important to state that, due to the geometrical circumstances of the penetrometer and because of manufacturing issues when making the steel plates, no round figures regarding hammer mass were obtained (hammer mass varied from a minimum value of 42.85 kg to a maximum value of 69.16 kg). The only criteria to be satisfied was to get hammer mass into this approximate range and mainly to know exactly the hammer mass and the height of fall in order to accurately calculate the nominal energy and then the $ENTHRU_{cone}$. It was not at all important to get round figures.

Fig. 11 Dynamic penetration apparatus and vehicle

Fig. 12 Dynamic penetrometer: amendment details
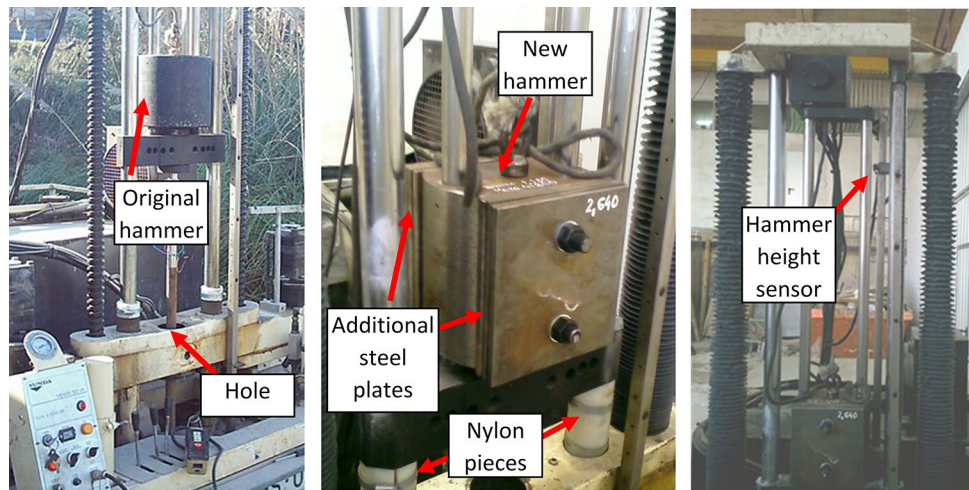
These possible hammer mass and height of fall values led us to nominal energies varying from approximately 150 to 500 J. As explained before, this is of the order of magnitude of usual DP tests in geotechnical practice (ISO-AENOR-CEN 2005, 2011; Matsumoto et al. 2015).

The penetrometer had also to be modified by adding a pair of nylon pieces in order to avoid the instrumented section being placed inside the hole that the penetrometer has in its frame (see Fig. 12).

Instrumentation and monitoring

The upper part of the rods was instrumented using four strain gauges and two accelerometers as can be seen in Figs. 13 and 14.

The instrumentation was located 32.6×10^{-2} m below the point of contact between the hammer and the anvil. This length was chosen in compliance with ISO-AENOR-CEN (2005, 2011). It is necessary that the instrumented section of rod be positioned at a distance greater than ten times the rod diameter below the point of hammer impact on the anvil.

Each of the four strain gauges was fixed and attached to the rod and was independent from the rest of the strain

gauges. They were assembled as four different quarter Wheatstone bridges.

The two ICP piezoelectric accelerometers were mounted diametrically opposite on small steel pieces that were bolted to the rod. The accelerometers were suitable for an acceleration of up to 10,000 g.

The signal conditioner/amplifier used in this research was the SCADAS III SC 316 front-end system signal acquisition equipment (from the LMS Difa Instruments Company).

Blows performed

The blows were performed in the shallowest layer of the soil where there were clean sands which were properly characterized. The blows were conducted at a very homogeneous part of the soil at two different depths: Zone 1 (from 2.5 to 3.2 m) and Zone 2 (from 4.6 to 5.2 m). Even though the clayey sands below 5.5–6.5 m (see soil resistivity profiles from Fig. 9) were not so well-identified and characterized, it was also decided to perform blows at these clayey sands in order to find out if the calculation of T_h depends on the type of soil, or not. The blows in these clayey sands were also conducted at a homogeneous part of this layer, i.e., Zone

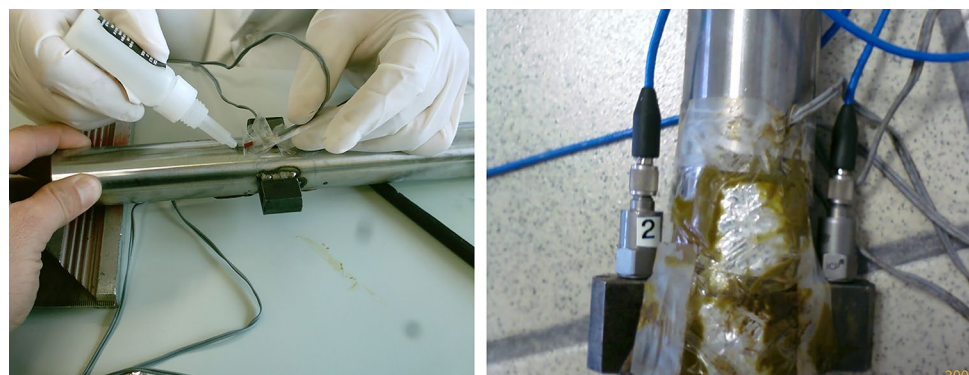**Fig. 13** Instrumented portion of the rod string: assembly

Fig. 14 Instrumented portion of the rod string with the strain gauges and the accelerometers

3 (from 6.7 to 7.0 m). These three different depths were chosen after the geotechnical and geophysical survey, with the three zones highlighted in the DPSH profiles shown in Fig. 15.

Since energy and penetration were needed to be obtained for every impact, a single blow (impact event) is defined as one complete test in this research.

At every impact event, acceleration and force were measured directly and independently, with the energy effectively transferred to the rods calculated as will be explained later.

In order to achieve T_h, as explained before, it is necessary to compare blows with different $ENTHRU_{cone}$. To this end, the nominal energy was changed from blow to blow. The mass of the hammer varied from a minimum value of 42.85 kg to a maximum value of 69.16 kg. The height of fall changed from 40 to 75 cm.

The values of the maximum torque for rod friction control T, measured at the three depths, were 5 N m, 13 N m, and 28 N m respectively. As expected, the greater the depth, the bigger the values of the maximum torque measured, due to the friction between the rods and the soil around them. These T values had to be used when calculating the $ENTHRU_{cone}$ as part of the input of Eq. (19).

Results and discussion

The importance of the processing of the signals from strain gages and accelerometers to get satisfactory results should be mentioned. Therefore, prior to the final results, we should explain and discuss some issues related to monitoring signals and their processing.

Interpretation and discussion of strain and acceleration signals

The first uncertainty, related to the signals from sensors, was to know if the signals registered were correct or not. That is why, besides the fact that the strain gauges and the accelerometers came ready-calibrated from the factory, before the tests, the whole of the monitoring assembly, including the sensors and the signal acquisition equipment, was fully calibrated by the authors in order to know if the measurements were correct. The measurements from the accelerometers

Fig. 15 DPSH-B penetration profiles
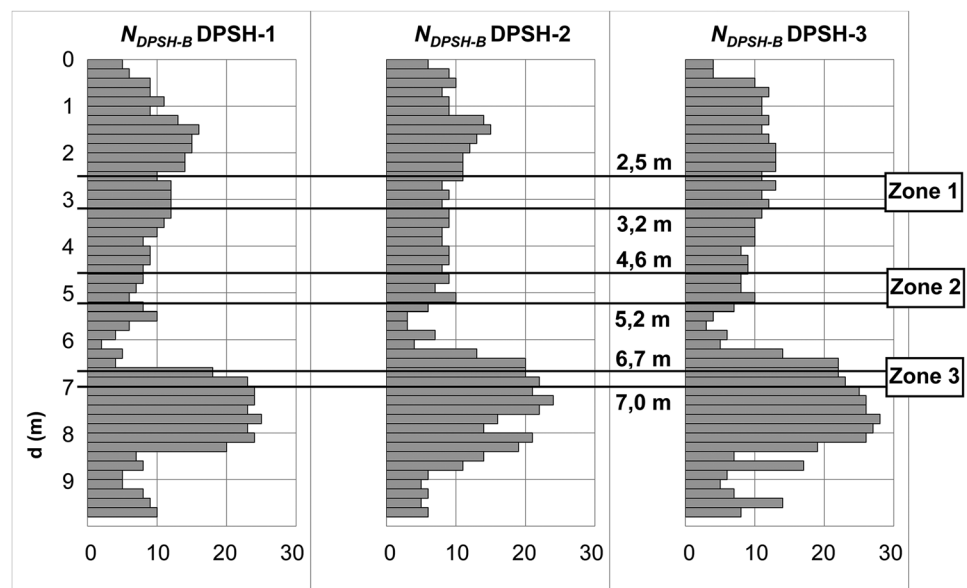
were calibrated by using a Brüel & Kjaer 4294/WH2606 calibration exciter, while the measurements from the strain gauges were calibrated by testing the instrumented rod in a loading frame via a compression test.

The signal conditioner/amplifier used in this research was SCADAS III signal acquisition equipment, model SC 316 front-end system (LMS Difa Instruments Company).

It was deemed important to connect the acquisition equipment and sensors in a way that minimized the noise signal. To ensure this, oxygen-free shielded cables were used, along with DB9 and LEMO connectors.

An anti-aliasing filter (low pass filter) was also used to minimize noise signal.

LMS Test.Lab 7B data acquisition software was used with a Signature Acquisition-RT interface.

Design oversampling digital data conversion at a rate of 25,600 Hz (sampling frequency) was employed with the final representation of the data at a rate of 10,000 Hz (frequency span). This was the goal for the rate, as sensors showed linear behavior up to this rate.

Data acquisition was designed to start 0.1 s before the impact where measured acceleration was greater than 50 g (noise signal could be up to 30 g). For acquisitions 0.1 s before the first impact, a pre-trigger had to be defined by the software.

One example of the records of these data is shown in Fig. 16 (blow 11: 2.64 m deep). The first impact is clearly visible in the direct records of force and acceleration, at a time of about 0.1 s, with a clear increase of about 300 J of the calculated transferred energy. At a time of about 0.15 s, a secondary (rebound) impact of much lower intensity is noticed, particularly in the acceleration.

The force was calculated using the elastic model (Eq. (28)), by averaging the value of the strain from the four strain gauges.

$$F = E \cdot \varepsilon \cdot A \tag{28}$$

where E represents the steel bar elastic modulus and ε is the strain.

The velocity was calculated by integrating (Eq. (29)) the acceleration signal from accelerometers in the time domain (an average value from the two accelerometer signals).

$$v = \int_0^t a \cdot dt \tag{29}$$

where a is the acceleration and t is the time.

Measuring energy and penetration

The method used in this research for measuring the *ENTHRU* was the FV, which measures the *EFV* (energy
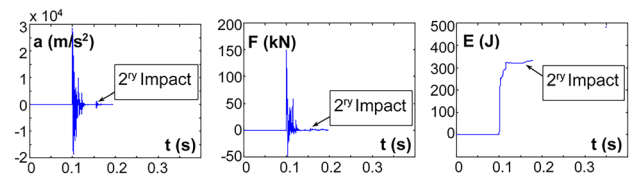

Fig. 16 Data from sensors and calculation of the energy effectively transferred to the rods

transmitted to the drill rod from the hammer during the impact event):

$$ENTHRU = \max \left[\int F(t) \cdot v(t) \cdot dt \right] \tag{30}$$

This is the method proposed in current standards (ASTM 2016; ISO-AENOR-CEN 2005, 2011).

The FV method is recommended instead of other methods that were used in the past, as many authors have proposed (Abou-Matar and Goble 1997; Butler et al. 1998; Farrar 1998; Sancio and Bray 2005; Schmertmann 2007; Sy and Campanella 1991).

It is important to note that *ENTHRU* is the maximum value of Eq. (30). *ENTHRU* is really calculated by integrating twice: firstly to get velocity from acceleration and secondly to calculate *ENTHRU* by applying Eq. (30). This mathematical issue can cause significant errors, mostly at the latter part of the records if there is noise signal. It is therefore essential to check every *ENTHRU* calculation. If *ENTHRU* does not remain as a constant value after the first and secondary impacts, the maximum value has to be computed after, while remaining close to the secondary impact.

Penetration was measured by means of a caliper, measured from a fixed part of the equipment (the method of integrating twice from acceleration values was discarded because of the increasing mathematical error).

The blows were performed with special care, as there are many variables that can adversely affect measured *ENTHRU*, such as lack of verticality, poor contact at joints, etc. (Reading et al. 2010), and the frequency of hammer blows (Seed et al. 1985).

Every integral was calculated using MATLAB software, aggregating the integrand in the time domain. By considering a discretization, the integral was transformed into an aggregation of finite addends (obtained from the values of the instrumented signals).

Results

The results from the blows are shown in Tables 1, 2, and 3.

Table 1 Experimental results at depths from 2.5 m to 3.2 m (Zone 1)

Blow	Depth (m)	m_h (kg)	h (cm)	p (mm)	E_n(J)	ENTHRU (J)	ENTHRU$_{cone}$ (J)	ENTHRU$_{cone}$/E_n	p^* (mm)
1	2.48	69.2	75	29.0	509	341	324	63.7%	15.9
2	2.51	63.9	75	20.0	470	340	326	69.3%	11.0
3	2.53	63.9	70	17.6	439	310	298	67.9%	9.7
4	2.54	63.9	65	16.4	408	297	285	69.9%	9.1
5	2.56	63.9	60	15.0	376	273	262	69.7%	8.3
6	2.58	63.9	55	14.2	345	239	229	66.4%	7.9
7	2.59	63.9	50	12.4	314	219	210	67.0%	6.9
8	2.60	63.9	45	11.3	282	202	194	68.8%	6.3
9	2.61	63.9	40	10.2	251	175	168	67.0%	5.7
10	2.63	63.9	75	17.9	470	339	326	69.2%	10.1
11	2.64	63.9	70	17.1	439	328	315	71.8%	9.6
12	2.66	63.9	65	16.1	408	293	281	69.0%	9.1
13	2.67	63.9	60	14.8	376	274	263	69.9%	8.4
14	2.69	63.9	55	13.8	345	250	240	69.5%	7.8
15	2.70	63.9	50	11.8	314	223	215	68.5%	6.7
16	2.71	63.9	45	11.3	282	205	197	69.7%	6.4
17	2.72	63.9	40	9.9	251	190	182	72.7%	5.6
18	2.74	63.9	75	17.4	470	346	333	70.8%	10.0
19	2.75	58.7	75	15.3	432	289	278	64.5%	8.8
20	2.77	53.4	75	13.5	393	270	261	66.4%	7.8
21	2.78	48.1	75	11.9	354	251	242	68.3%	6.9
22	2.79	42.9	75	10.5	315	226	218	69.1%	6.1
23	2.81	69.2	75	17.2	509	313	302	59.4%	9.9
24	2.82	63.9	75	15.3	470	316	305	64.9%	8.9
25	2.84	58.7	75	14.1	432	286	277	64.1%	8.2
26	2.85	53.4	75	12.8	393	277	267	68.0%	7.5
27	2.86	48.1	75	11.2	354	248	240	67.8%	6.5
28	2.87	42.9	75	9.6	315	228	220	69.9%	5.6
29	2.96	63.9	75	14.7	470	321	310	66.0%	8.7
30	2.98	58.7	70	12.8	403	272	263	65.3%	7.6
31	3.01	53.4	65	10.6	341	234	226	66.4%	6.3
32	3.02	53.4	60	10.1	314	214	207	65.7%	6.0
33	3.04	53.4	55	9.4	288	198	191	66.3%	5.6
34	3.04	53.4	50	8.5	262	183	177	67.6%	5.1
35	3.05	48.1	45	7.4	212	163	157	74.0%	4.4
36	3.06	42.9	40	5.6	168	133	128	76.4%	3.4
37	3.07	63.9	75	14.9	470	301	292	62.0%	9.0
38	3.08	58.7	70	12.4	403	255	247	61.3%	7.5
39	3.09	53.4	65	10.4	341	230	223	65.3%	6.3
40	3.10	53.4	60	9.7	314	215	208	66.2%	5.9
41	3.11	53.4	55	9.5	288	208	201	69.6%	5.8
42	3.12	53.4	50	8.9	262	188	181	69.1%	5.4
43	3.13	48.1	45	6.9	212	158	153	71.9%	4.2
44	3.15	42.9	40	5.7	168	126	122	72.5%	3.5

The value of T_h was calculated at these three different depths, in line with the previously explained. A statistical analysis is also required in order to verify the main hypothesis in this research, i.e., the existence of an apparent T_h if a linear correlation is used to compare results from various kinds of penetration tests.

Table 2 Experimental results at depths from 4.6 to 5.2 m (Zone 2)

Blow	Depth (m)	m_h (kg)	h (cm)	p (mm)	E_n(J)	ENTHRU (J)	ENTHRU$_{cone}$ (J)	ENTHRU$_{cone}$/E_n	p* (mm)
1	4.59	63.9	75	19.2	470	338	301	64.1%	14.3
2	4.60	42.9	40	6.6	168	143	128	76.1%	4.9
3	4.79	63.9	75	17.8	470	306	275	58.5%	13.5
4	4.80	42.9	75	11.5	315	237	214	67.7%	8.7
5	4.82	63.9	75	18.3	470	313	281	59.6%	13.9
6	4.83	63.9	40	10.8	251	187	165	65.9%	8.2
7	4.85	63.9	75	19.1	470	350	312	66.2%	14.6
8	4.86	42.9	40	7.2	168	133	118	70.2%	5.5
9	4.87	63.9	75	19.7	470	352	312	66.4%	15.1
10	4.89	42.9	75	12.4	315	246	219	69.6%	9.5
11	4.91	63.9	75	19.4	470	342	304	64.7%	14.9
12	4.92	63.9	40	11.4	251	199	175	69.6%	8.8
13	4.94	63.9	75	19.4	470	338	300	63.9%	14.9
14	4.95	42.9	40	7.0	168	135	120	71.3%	5.4
15	4.96	63.9	75	18.6	470	337	301	64.0%	14.4
16	4.98	42.9	75	12.0	315	243	218	69.1%	9.3
17	4.99	63.9	75	18.5	470	325	290	61.8%	14.3
18	5.01	63.9	40	11.0	251	188	166	66.3%	8.5
19	5.02	63.9	40	10.6	251	188	167	66.6%	8.2
20	5.03	63.9	75	18.3	464	353	315	67.9%	14.2
21	5.05	63.9	75	18.3	470	347	310	66.0%	14.2
22	5.07	63.9	70	17.5	439	321	287	65.3%	13.6
23	5.09	63.9	65	16.9	408	297	264	64.8%	13.2
24	5.10	63.9	60	16.2	376	291	257	68.3%	12.7
25	5.15	63.9	55	12.0	345	261	236	68.5%	9.4
26	5.17	63.9	50	9.5	314	230	210	67.0%	7.5
27	5.19	63.9	45	7.8	282	205	189	66.9%	6.1

Values of energy threshold

At every aforementioned zone, the results were plotted in a separate graph, as shown in Figs. 17, 18, and 19.

First blows were performed using many different nominal energy values, which is why, in Fig. 17, there are tests with many different ENTHRU$_{cone}$ values. For operative reasons, the next blows were mostly conducted by using only four different nominal energies, which explains why, at deeper locations and especially in Fig. 19, most of the points are concentrated closer together at certain ranges.

T_h is the *x*-intercept of these correlation lines of best fit in Figs. 17, 18, and 19. The results can be seen in Table 4.

It is important to remark that there is not a single, universal value for this threshold: T_h depends on the nature of the soil and the type of DP test (regarding the cross-sectional area of the cone).

Analysis of the elastic stiffness of the soil

The value of *k* was calculated for the three different zones under study, according to Eq. (27) and Fig. 5. These results are summarized in Table 5.

By knowing the value of C_N, the ultimate driving resistance (R_u) was calculated (see Table 5). Figure 20 shows the values of R_u for the three studied zones. As expected, there is an apparent tendency to increase with the soil penetration resistance (N_{DPSH-B}), regardless of the depth (the influence of the depth has been eliminated by using the factor C_N (Eq. (22)).

The value of *k* is similar for the clean sand (Zones 1 and 2) and higher for the clayey sand (Zone 3).

Statistical analysis

The theoretical equation for the linear model in the regression analysis that has been done is as follows (see Figs. 1 and 5):

$$p* = m_E \cdot ENTHRU_{cone} - m_E \cdot T_h \tag{31}$$

where m_E is the slope and $-m_E \cdot T_h$ is the *y*-intercept in this linear model.

This factor m_E, which is the incremental ratio between penetration and effective energy, is a measure of the reciprocal of $R_u \cdot C_N$ (see Fig. 5).

Table 3 Experimental results at depths from 6.7 to 7.0 m (Zone 3)

Blow	Depth (m)	m_h (kg)	h (cm)	p (mm)	E_n(J)	ENTHRU (J)	ENTHRU$_{cone}$ (J)	ENTHRU$_{cone}$/E_n	p^* (mm)
1	6.73	63.9	75	9.6	470	366	318	67.6%	8.6
2	6.74	42.9	40	3.6	168	142	123	73.1%	3.2
3	6.74	63.9	75	9.1	470	355	310	66.0%	8.1
4	6.75	42.9	75	5.5	315	253	224	71.1%	4.9
5	6.76	63.9	75	8.6	470	351	309	65.7%	7.7
6	6.76	63.9	40	4.9	251	202	176	70.2%	4.4
7	6.77	63.9	75	8.4	470	361	318	67.7%	7.5
8	6.78	42.9	40	2.9	168	144	127	75.7%	2.6
9	6.78	63.9	75	8.1	470	348	309	65.6%	7.2
10	6.79	42.9	75	5.0	315	254	227	71.9%	4.5
11	6.80	63.9	75	8.5	470	353	311	66.2%	7.6
12	6.80	63.9	40	4.3	251	209	185	73.7%	3.9
13	6.81	63.9	75	8.0	470	351	312	66.2%	7.2
14	6.81	42.9	40	2.7	168	143	127	75.7%	2.4
15	6.82	63.9	75	7.7	470	355	316	67.2%	6.9
16	6.83	42.9	75	5.0	315	255	228	72.2%	4.5
17	6.83	63.9	75	7.6	470	353	315	67.0%	6.8
18	6.84	63.9	40	4.6	251	204	180	71.6%	4.1
19	6.84	63.9	75	7.4	470	358	320	68.1%	6.6
20	6.85	42.9	40	2.6	168	146	130	77.6%	2.3
21	6.85	63.9	75	7.4	470	354	316	67.3%	6.7
22	6.86	42.9	75	4.9	315	262	235	74.4%	4.4
23	6.87	63.9	75	7.4	470	355	317	67.5%	6.7
24	6.87	63.9	40	4.3	251	206	182	72.7%	3.9
25	6.88	63.9	75	7.4	470	351	314	66.8%	6.7
26	6.88	42.9	40	2.7	168	145	130	77.1%	2.4
27	6.89	63.9	75	7.3	470	352	315	66.9%	6.6
28	6.89	42.9	75	4.9	315	253	226	71.7%	4.4
29	6.90	63.9	75	7.2	470	347	311	66.2%	6.5
30	6.91	63.9	40	4.0	251	205	183	73.0%	3.6
31	6.91	63.9	75	7.2	470	354	317	67.4%	6.5
32	6.92	42.9	40	2.7	168	142	127	75.6%	2.4
33	6.92	63.9	75	7.2	470	346	310	66.0%	6.5
34	6.93	42.9	75	4.7	315	236	212	67.2%	4.2
35	6.93	63.9	75	7.2	470	349	312	66.4%	6.5
36	6.94	63.9	40	4.0	251	201	180	71.6%	3.6
37	6.95	63.9	75	7.2	470	353	317	67.3%	6.5

T_h is the x-intercept (see Figs. 1 and 5).

When using a linear trending line to interpolate, as in this case, it is easy to calculate the statistical parameters of the slope and the y-intercept. In every line, the x-intercept (in this case T_h), the slope (m_E), and the y-intercept ($-m_E \cdot T_h$) fulfil the next relationship:

$$x - \text{intercept} = -\frac{y - \text{intercept}}{\text{slope}} \tag{32}$$

The sampling standard deviation of the x-intercept, i.e., the standard deviation of T_h (S_{Th}), can therefore be expressed in terms of the sampling variances and the mean values of the slope (m_E) and the y-intercept ($-m_E \cdot T_h$):

$$S_{T_h} = \overline{T_h} \cdot \sqrt{\frac{S^2_{-m_E \cdot T_h}}{\overline{-m_E \cdot T_h}^2} + \frac{S^2_{m_E}}{\overline{m_E}^2}} \tag{33}$$
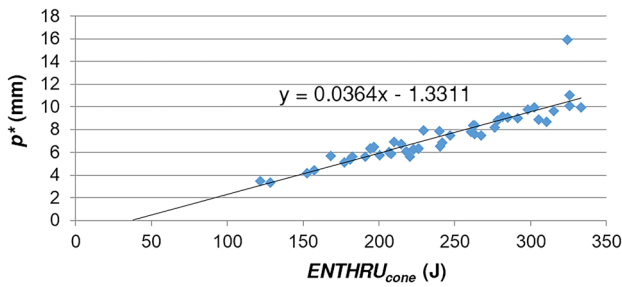
Fig. 17 $ENTHRU_{cone}$ vs. p^* at Zone 1 (depths from 2.5 to 3.2 m)

where S^2 is the sampling variance (COV).

The correlation coefficient (R) of the linear model in this simple regression calculations and the summary of the results of the previous equations is shown in Table 6. Statgraphics Plus 4.0 software was used.

The P-value in the ANOVA analysis is 0.0000 for the three cases studied at the three depths considered.

Discussion

Since the P-value in the ANOVA analysis is less than 0.01, there is a statistically significant relationship between $ENTHRU_{cone}$ and p/C_N at the 99% confidence level.

Similarly, the correlation coefficients (R), as seen in Table 6, indicate a strong relationship between the variables. Values of R and R^2 are high enough, even though not any outlier has been discarded from this research, unlike some authors (Viviescas et al. 2019) that have proven to be reasonable to exclude some SPT outliers for researching. Obviously, discarding outliers would have even increased the values of R and R^2.

The sampling standard deviation of T_h (S_{Th}), which is not higher than the value of T_h, indicates that T_h probably exists statistically, with a positive value.

The results from the tests are clear: the soil behaves as if it were needed to subtract T_h from $ENTHRU_{cone}$ to properly correlate the real penetrations and the blow count between different penetration tests.
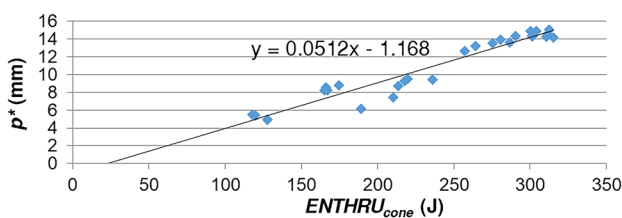

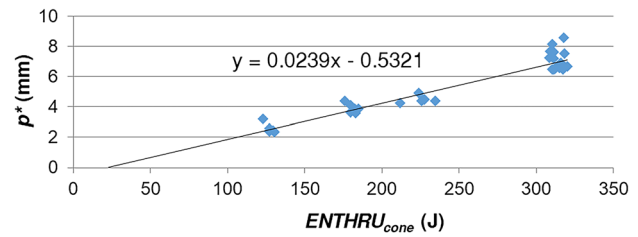**Fig. 18** $ENTHRU_{cone}$ vs. p^* at Zone 2 (depths from 4.6 to 5.2 m)

Equation (20) should then be expressed thus:

$$N_1 = N_2 \cdot \frac{ENPEN_2 \cdot A_1 \cdot e_1}{ENPEN_1 \cdot A_2 \cdot e_2} \tag{34}$$

This behavior should clearly be quite different for very low nominal energies, although it does work for the usual nominal energies in the most common penetration tests. These regression lines should evidently start from the origin of the coordinate system (if there is no penetration at all, the energy measured should be zero). For lower energy values, regression lines should therefore be curved, as shown in Fig. 1. However, for the usual energy values used in DP tests, the soil actually behaves as if there was a linear relationship between energy and penetration, but with an apparent energy threshold (T_h), as explained in Figs. 1 and 5. Nevertheless, it is important to emphasize that, even though the values of these T_h are not particularly high, they cannot be considered negligible (in this case, the values were always greater than 20 J).

In this research, the method of calculating this T_h is by means of plotting graphs as in Figs. 17, 18, and 19, although it could be easily approximately calculated by applying Eq. (27).

R_u can be calculated by using the Hiley formula for pile capacity (Hiley 1925), adapted for penetration testing. Thus, assuming the temporary elastic compressions vanish, the Hiley formula is as follows:

$$R_u = \frac{m_h}{m_h + m_a + m_r} \cdot \frac{m_h \cdot g \cdot h}{e/N} \tag{35}$$

where N is the number of blows in a penetration test.

The soil elastic stiffness (k) can be calculated by using the modulus of subgrade reaction (K):

Fig. 19 $ENTHRU_{cone}$ vs. p^* at Zone 3 (depths from 6.7 to 7.0 m)

Table 4 Values of T_h

Zone	T_h (J)
Zone 1	37
Zone 2	23
Zone 3	22

Table 5 Elastic stiffness (k)

Zone	N_{DPSH-B}	$1/(R_u \cdot C_N)$	C_N	R_u (kN)	T_h (J)	k (kN/m)
Zone 1	10.5	0.0364	1.727	16	37	3420
Zone 2	8	0.0512	1.299	15	23	4915
Zone 3	20.5	0.0239	1.113	38	22	32119
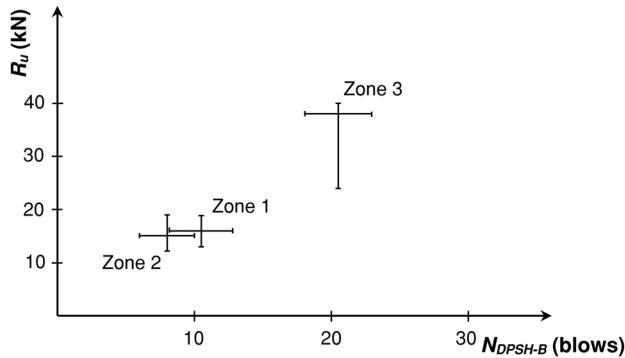
Fig. 20 Ultimate driving resistance (R_u) vs. Penetration resistance (N_{DPSH-B})

$$q = K \cdot s \tag{36}$$

where q is the applied pressure.

If we want to calculate the force:

$$F = K \cdot s \cdot A \tag{37}$$

Comparing to Eq. (24), we obtain the equation for calculating the soil elastic stiffness (k):

$$k = K \cdot A \tag{38}$$

The value of K can be calculated by using (Muzás Labad 2002; Terzaghi 1955) the next equation (for submerged sands):

$$K_{30}\left(kg/cm^3\right) = 0.6 \cdot 10^{\frac{N_{SPT}+2}{34}} \tag{39}$$

where K_{30} is the subgrade reaction coefficient corresponding to a 30 cm diameter and N_{SPT} is the number of blows obtained when conducted a SPT test.

In order to correlate N_{SPT} and N_{DPSH-B}, we can apply this equation (Ibanez 2009):

$$N_{SPT} = 2 \cdot N_{DPSH-B} \tag{40}$$

K can then be calculated through the current formula for sands (Muzás Labad 2002; Terzaghi 1955):

$$K = K_{30} \cdot \left(\frac{d_c(m) + 0.3}{2 \cdot d_c(m))} \right)^2 \tag{41}$$

where d_c is the diameter of the cone in meters.

If we apply these last equations for the results obtained through this investigation, we obtain the values of R_u, k, and then T_h (Eq. (27)). These results are shown in Table 7.

The results of T_h are enough similar to those of Table 5, so we can assume this manner of calculating T_h can be appropriate.

As was demonstrated (Figs. 17, 18, and 19), the soil actually behaves as if there were a linear relationship between energy and penetration beyond that T_h, with the penetration closely related to such *ENPEN* (Eq. (21)). It would clearly be interesting to propose a new method for calculating the energy correction required to adjust the blow counts to 60% energy efficiency (N_{60}) by using a correction who includes this T_h:

$$N_{60} = \frac{\eta \cdot m_h \cdot g \cdot h - T_h}{0.60 \cdot m_h \cdot g \cdot h - T_h} \cdot N \tag{42}$$

Table 7 R_u, k, and T_h calculation

Zone	R_u (kN)	k (kN/m)	T_h (J)
Zone 1	17	2925	49
Zone 2	10	1090	48
Zone 3	19	8403	22

Table 6 Statistical results

Zone	T_h (J)	R	m_E	$-m_E \cdot T_h$	S_{mE}	$S_{-mE \cdot Th}$	S_{Th} (J)
Zone 1	37	0.8992	0.0364	-1.3311	0.0027	0.6718	19
Zone 2	23	0.9629	0.0512	-1.1684	0.0029	0.7089	14
Zone 3	22	0.9595	0.0239	-0.5321	0.0012	0.3060	13

Conclusions

In order to calculate penetrations in DP tests (as well as in SPT tests), it is necessary to use $ENTHRU_{cone}$ instead of $ENTHRU$, as the energy that really produces penetration is the fraction of the total energy that effectively reaches the tip of the cone below the rod string.

The way of measuring energy in dynamic probing (DP tests) is different from that used in SPT tests, which is mainly due to the existence of skin friction between the drive rods and the soil around them.

In order to calculate $ENTHRU_{cone}$ in DP tests, a new equation (Eq. (19)) is proposed while to calculate $ENTHRU_{cone}$ correctly, it is necessary to measure $ENTHRU$ using an instrumented rod. In DP tests, it is not enough accurate to calculate $ENTHRU$ by means of equations similar to Eq. (15), because of the additional difficulty of calculating the possible values of energy efficiency factors.

It has been proved that soil actually behaves as if there were a certain amount of energy (T_h) to be exceeded by $ENTHRU_{cone}$, to produce penetration. For the usual energy values used in DP tests (the range of real interest), the soil behaves as if there were a linear relationship between energy and penetration, but with a virtual energy threshold (T_h). The values of these T_h are not negligible (greater than 20 J in this case).

In order to correlate results from different DP tests (e.g., by using Eq. (20)), it is desirable the use of $ENPEN$ (Eq. (21)), instead of $ENTHRU$ or $ENTHRU_{cone}$, and definitely the use of $ENPEN$ (Eq. (34)) is considerably more appropriate than using nominal energies, as it is usual practice when applying Eq. (20). This new proposed and improved way of correlating results among various kinds of dynamic penetration tests requires the calculation of T_h, which can be obtained by means of Eq. (27).

As the soil actually behaves as if there were a linear relationship between energy and penetration beyond that T_h, a new method for calculating the energy correction required to adjust the blow counts to 60% energy efficiency (via Eq. (42)) is also proposed.

References

Abou-Matar H, Goble GG (1997) SPT dynamic analysis and measurements. J Geotech Geoenviron Eng 123:921–928. https://doi.org/10.1061/(ASCE)1090-0241(1997)123:10(921)

Anbazhagan P, Kumar A, Ingale SG, Jha SK, Lenin KR (2021) Shear modulus from SPT N-values with different energy values. Soil Dyn Earthq Eng 150:106925. https://doi.org/10.1016/j.soildyn.2021.106925

Anbazhagan P, Yadhunandan ME, Kumar A (2022) Effects of hammer energy on borehole termination and SBC calculation through site-specific hammer energy measurement using SPT HEMA. Indian Geotech J. https://doi.org/10.1007/s40098-021-00582-z

ASTM (2016) D4633–16: Standard Test Method for Energy Measurement for Dynamic Penetrometers. ASTM, Conshohocken, PA

Avanzi GDA, Galanti Y, Giannecchini R, Lo Presti D, Puccinelli A (2013) Estimation of soil properties of shallow landslide source areas by dynamic penetration tests: first outcomes from Northern Tuscany (Italy). Bull Eng Geol Environ 72:609–624. https://doi.org/10.1007/s10064-013-0535-y

Bergdahl U (1979) Development of the dynamic probing test method. Design parameters in geotechnical engineering. BGS, London, pp 201–206

Briaud J-L (2013) Geotechnical engineering: unsaturated and saturated soils. John Wiley & Sons Inc, Hoboken, New Jersey

Butler J, Caliendo J, Goble G (1998) Comparison of SPT energy measurement methods. 1st Int Conf on Site Characterization, Atlanta, pp 901–905

Cearns P, McKenzie A (1988) 12. Application of dynamic cone penetrometer testing in East Anglia. Penetration testing in the UK: Geotechnology Conference Penetration Testing in the UK, organized by the Institution of Civil Engineers. Thomas Telford Publishing, Birmingham, pp 123–127

Dahlberg R, Bergdahl U (1974) Investigations on the Swedish ramsounding method. European Symposium on Penetration Testing, Stockholm, pp 93–101

Daniel CR, Howie JA, Jackson RS, Walker B (2005) Review of standard penetration test short rod corrections. J Geotech Geoenviron Eng 131:489–497. https://doi.org/10.1061/(asce)1090-0241(2005)131:4(489)

Daniel CR, Howie JA, Sy A (2003) A method for correlating large penetration test (LPT) to standard penetration test (SPT) blow counts. Can Geotech J 40:66–77. https://doi.org/10.1139/T02-094

Danziger FA, Danziger BR, Cavalcante EH (2006) Discussion of "Review of standard penetration test short rod corrections" by Chris R. Daniel, John A. Howie, R. Scott Jackson, and Brian Walker. J Geotech Geoenviron Eng 132:1634–1637. https://doi.org/10.1061/(ASCE)1090-0241(2006)132:12(1634)

Farrar J (1998) Summary of Standard Penetration Test (SPT) energy measurement experience. Proc 1st Int Conf on Site Characterization, Atlanta, pp 919–926

Hiley A (1925) A rational pile-driving formula and its appliation in piling practice explained. Engineering 657:721

Housel WS (1965) Michigan study of pile driving hammers. J Soil Mech Found Div 91:37–64

Ibanez SJ (2009) Análisis de ensayos de penetración dinámica a través de su rendimiento energético. Universidad de Cantabria (PhD. Thesis)

Ibanez SJ, Sagaseta C, Lopez-Ausin V (2012) Measuring energy in dynamic probing. 4th International Conference on Geotechnical and Geophysical Site Characterization, ISC´4, Porto de Galinhas, Brazil. Volume 1:399–404

ISO-AENOR-CEN (2005, 2011) ISO 22476–2:2005: Geotechnical investigation and testing-Field testing-Part 2: Dynamic probing, and ISO 22476-2:2005/Amendment 1: 2011. Switzerland, Geneva

Kovacs WD, Salomone LA (1982) SPT hammer energy measurement. J Geotech Eng Div 108:599–620

Lancellota R (1995) Geotechnical Engineering. A.A. Balkema, Rotterdam/Brookfield

Lee C, An S, Lee W (2014) Real-time monitoring of SPT donut hammer motion and SPT energy transfer ratio using digital line-scan camera and pile driving analyzer. Acta Geotech 9:959–968. https://doi.org/10.1007/s11440-012-0197-0

Lee C, Lee J-S, An S, Lee W (2009) Effect of secondary impacts on SPT rod energy and sampler penetration. J Geotech Geoenviron Eng 136:522–526. https://doi.org/10.1061/(ASCE)GT.1943-5606.0000236

Lee M-J, Hong S-J, Kim R, Chae Y-H, Lee W (2012) Evaluation of cementation of Jeju coastal sediments using in situ tests. Bull Eng Geol Environ 71:511–518. https://doi.org/10.1007/s10064-012-0425-8

Liao SS, Whitman RV (1986) Overburden correction factors for SPT in sand. J Geotech Eng 112:373–377. https://doi.org/10.1061/(ASCE)0733-9410(1986)112:3(373)

Look B, Seidel J, Sivakumar S, Welikala D (2015) Real time monitoring of SPT using a PDM device–The Failings of our Standard Test revealed. International Conference on Geotechnical Engineering, Colombo, Sri Lanka

Lukiantchuki JA, Bernardes GP, Esquivel ER (2017) Energy ratio (E-R) for the standard penetration test based on measured field tests. Soils Rocks 40:77–91. https://doi.org/10.28927/sr.402077

Matsumoto T, Phan LT, Oshima A, Shimono S (2015) Measurements of driving energy in SPT and various dynamic cone penetration tests. Soils Found 55:201–212. https://doi.org/10.1016/j.sandf.2014.12.016

Michi Y, Matsumoto T, Ishihara S, Shirai N (2004) Application of dynamic portable cone penetration tests to quality assessment of improved soil. Proceedings, Seventh International Conference on the Application of Stress-Wave Theory to Piles, pp 333–340

Mishra S, Robinson RG (2019) Laboratory investigation on quasi-static penetration testing using SPT sampler in soft clay bed. Geotech Test J 42:985–1005. https://doi.org/10.1520/gtj20170127

Muzás Labad F (2002) Considerations regarding the selection of coefficients of subgrade reaction (Consideraciones sobre la elección de coeficientes de balasto). Revista de Obras Públicas, pp 45–51

NBR-ABNT (2001) 6484: Sondagens de Simples Reconhecimento com SPT-Método de Ensaio. CB-02, Rio de Janeiro

Nixon I (1988) Introduction to Papers 10–13. Penetration testing in the UK: Proceedings of the Geotechnology Conference Penetration Testing in the UK, organized by the Institution of Civil Engineers. Thomas Telford Publishing, Birmingham, pp 105–111

Odebrecht E, Schnaid F, Rocha MM, de Paula BG (2005) Energy efficiency for standard penetration tests. J Geotech Geoenviron Eng 131:1252–1263. https://doi.org/10.1061/(ASCE)1090-0241(2005)131:10(1252)

Palacios A (1977) The theory and measurement of energy transfer during standard penetration test sampling. University of Florida (PhD. Thesis)

Pazdirek O, Blaha V (1996) Examples of resistivity imaging using ME-100 resistivity field acquisition system. 58th EAGE Conference and Exhibition. European Association of Geoscientists & Engineers, p cp-48-00228

Reading P, Lovell J, Spires K, Powel J (2010) The implications of the measurement of energy ratio (Er) for the Standard Penetration Tests. Ground Eng 43:28–31

Sancio RB, Bray JD (2005) An assessment of the effect of rod length on SPT energy calculations based on measured field data. Geotech Test J 28:1–9

Scarff R (1988) Factors governing the use of continuous dynamic probing in UK ground investigation. In: Casin M (ed) Penetration testing in the UK: Proceedings of the Geotechnology Conference Penetration Testing in the UK, organized by the Institution of Civil Engineers. Thomas Telford Publishing, Birmingham, pp 129–132

Schmertmann JH (2007) Discussion of "Energy Efficiency for Standard Penetration Test" by Edgar Odebrecht, Fernando Schnaid, Marcelo Maia Rocha, and George de Paula Bernardes. J Geotech Geoenviron Eng 133:487–488. https://doi.org/10.1061/(ASCE)1090-0241(2007)133:4(487)

Schmertmann JH, Palacios A (1979) Energy dynamics of SPT. J Geotech Eng Div 105:909–926

Seed HB, Tokimatsu K, Harder L, Chung RM (1985) Influence of SPT procedures in soil liquefaction resistance evaluations. J Geotech Eng 111:1425–1445

Soriano A (1994) Hinca dinámica y control. CEDEX, Madrid, Spain

Sy A, Campanella RG (1991) An alternative method of measuring SPT energy. 2nd International Conference on Recent Advances in Geotechnical Earthquake Engineering and Soil Dynamics, St. Louis, Missouri, USA, pp 499–505

Terzaghi K (1955) Evalution of coneficients of subgrade reaction. Geotechnique 5:297–326

Viviescas JC, Osorio JP, Griffiths DV (2019) Cluster analysis for the determination of the undrained strength tendency from SPT in mudflows and residual soils. Bull Eng Geol Environ 78:5039–5054. https://doi.org/10.1007/s10064-019-01472-8

Žaržojus G, Kelevišius K, Amšiejus J (2013) Energy transfer measuring in dynamic probing test in layered geological strata. 11th International Scientific Conference on Modern Building Materials, Structures and Techniques (MBMST), Vilnius, Lithuania, pp 1302–1308